Article

Not peer-reviewed version

An Innovative Bioremediation Approach to Heavy Metal Removal: Combined Application of *Chlorella vulgaris* and amin functionalized $MgFe_2O_4$ Nanoparticles in Industrial Wastewater Treatment

Timea Foris , Peter Koska , Agnes Maria Ilosvai , Ferenc Kristály , Lajos Daroczi , Laszlo Vanyorek , Bela Viskolcz *

Posted Date: 12 May 2025

doi: 10.20944/preprints202505.0828.v1

Keywords: *Chlorella vulgaris*; heavy metal adsorption; amine-functionalized magnesium ferrite

 doi:10.20944/preprints202505.0828.v1

Article

An Innovative Bioremediation Approach to Heavy Metal Removal: Combined Application of Chlorella vulgaris and amin functionalized $MgFe_2O_4$ Nanoparticles in Industrial Wastewater Treatment

Tímea Fóris [1], Péter Koska [1,2], Ágnes Maria Ilosvai [1,2], Ferenc Kristály [3], Lajos Daróczi [4], László Vanyorek [1] and Béla Viskolcz [1,2]

[1] Institute of Chemistry, University of Miskolc, Miskolc-Egyetemváros, 3515 Miskolc, Hungary; timea.foris1@uni-miskolc.hu

[2] Higher Education and Industrial Cooperation Centre, University of Miskolc, 3515 Miskolc, Hungary; peter.zoltan.koska@uni-miskolc.hu

[3] Institute of Mineralogy and Geology, University of Miskolc, 3515 Miskolc-Egyetemváros, Hungary; askkf@uni-miskolc.hu

[4] Department of Solid State Physics, University of Debrecen, P.O. Box 2, 4010 Debrecen, Hungary; lajos.daroczi@science.unideb.hu

* Correspondence: bela.viskolcz@uni-miskolc.hu

Abstract: The removal of heavy metals from industrial wastewater remains a major environmental challenge, demanding efficient, sustainable solutions. This study explores the combined use of Chlorella vulgaris and amine-functionalized magnesium ferrite ($MgFe_2O_4$-NH_2) nanoparticles to remove cobalt ions from battery effluents. The research aims to explore the capacity of *C. vulgaris* to adsorb heavy metals, followed by their separation using magnetic nanoparticles. Cobalt adsorption by *C. vulgaris* was facilitated through the interaction of metal ions on the cell wall, achieving a removal efficiency of 96.44% within 30 minutes, which increased to 98.78% over 10 hours. Amine-functionalized $MgFe_2O_4$ nanoparticles, synthesized and characterized using HRTEM, FTIR, and VSM, displayed high surface reactivity due to the presence of -NH_2 and -OH groups. At neutral pH, zeta potential measurements revealed a slightly negative charge (-5.6 ± 4.3 mV), while protonation at lower pH levels enhanced electrostatic interactions with the negatively charged algal biomass. Magnetic separation of the cobalt-adsorbed biomass achieved efficiencies ranging from 94.9% to 99.2% within 60 seconds, significantly outperforming conventional sedimentation methods. SEM and FTIR analyses confirmed the binding of nanoparticles to algal cell walls. The even distribution of $MgFe_2O_4$ nanoparticles on algal surfaces was further validated by TEM imaging, and the strong magnetic properties of the nanoparticles enabled rapid and efficient separation under an external magnetic field.

Keywords: Chlorella vulgaris; heavy metal adsorption; amine-functionalized magnesium ferrite;

1. Introduction

The contamination of natural waters and soil with heavy metals from industrial effluents represents a significant environmental concern in the present era. The battery industry represents a significant source of heavy metal contamination, with industrial wastewater from battery manufacturing and recycling companies containing considerable quantities of heavy metals. The cathode of Li-batteries produced for the automotive industry (e.g. NMC, NCA, LMO cells) contains nickel, manganese and cobalt metals in varying proportions [1]. At higher concentrations, heavy metal pollution is dangerous because of its direct toxic effects on living organisms; however, at low concentrations it also poses a serious risk due to its accumulation in the food chain [2]. Several

 doi:10.20944/preprints202505.0828.v1

technologies have been developed to remove heavy metals from industrial wastewater, including ion exchange, reverse osmosis, electrodialysis and ultrafiltration [3]. However, in addition to their efficiency, these processes often present several disadvantages, including incomplete metal removal, sludge formation, high reagent and energy requirements, metal precipitate aggregation, and fouling of membrane filters. In consequence, alternative technologies have emerged as a significant area of research in recent years. Among these, bioremediation processes have attracted particular attention as a treatment technology for the removal of heavy metals [4]. This interest stems from technology's perceived economic feasibility, efficiency, and environmental compatibility [5].

Bioremediation processes encompass technologies that utilise biological systems to diminish the concentration and detrimental effects of pollutants to an acceptable level. The main organisms used in bioremediation technologies are microorganisms, including bacteria, algae and yeasts [6]. These can adsorb toxic metal ions on their cell surfaces, accumulating them in large amounts in the intracellular space [7]. *Chlorella vulgaris*, a freshwater microalga, has been identified as a particularly efficacious agent in this regard [8]. The cell wall of Chlorella vulgaris is composed of complex carbohydrates, with a network of cellulose fibres attached to a variety of polysaccharides, including hemicellulose and glycoproteins [9]. Furthermore, monosaccharides (e.g. glucose, mannose, galactose, xylose, fucose, arabinose), lipids and considerable quantities of glucosamines are present. The functional groups present in these polymer molecules are significant regarding the processes of adsorption. The cell wall biopolymer was found to contain several functional groups, including carboxyl (-COOH), hydroxyl (-OH), amino ($-NH_2$), carbonyl (-C=O), ester (-CO-O), sulfhydryl (-SH), sulfate ($-SO_4^{2-}$) and phosphate (PO_4^{3-}). The functional groups are protonated in accordance with the pH level, thereby influencing the charge of the cell wall [10]. It can be observed that above pH 3, the negative charge of carboxyl groups, phosphate groups and hydroxyl groups is predominant, with positively charged heavy metal cations adsorbing to the negatively charged cell wall [11]. The adsorption of cell surface biopolymers can occur by several mechanisms, including physisorption, ion exchange, chelation and complexation [12].

In addition to the removal of heavy metal ions from industrial wastewater, the issue of how to remove algae that accumulates heavy metal ions from wastewater must be addressed. Several conventional methods have been developed for the removal of algae from wastewater. The most used methods are sedimentation, flotation, coagulation and flocculation, filtration, and sedimentation [13]. Magnetic separation is an innovative technology that is characterised by rapidity, cost-effectiveness and energy efficiency. Algal cells exhibit a high affinity for the adsorption of magnetisable nanoparticles (MNPs) onto the surface of their cell walls, thereby enabling their isolation from wastewater in a magnetic field of sufficient strength [14,15]. The conventional sedimentation method took more than 2 hours for the coagulation and settling of algae, whereas the magnetic separation technique achieved the same outcome in just 30 seconds [16]. Both naked and surface-functionalized (using polyacrylamides, chitosan, poly diallyldimethylammonium chloride (PDDA), aminoclay, polyethylenimine (PEI), 3-aminopropyl triethoxysilane (APTES)) magnetic nanoparticles have been applied for the harvesting of *C. vulgaris* [17–23]. Specifically, amine-functionalized $MgFe_2O_4$ nanoparticles exhibit high efficiency in binding to cell walls rich in negatively charged carboxyl groups [24]. Furthermore, magnetic biomass can be rapidly and efficiently separated by applying an external magnetic field, facilitating streamlined recovery and reuse.

The purpose of this study is to examine the capacity of *Chlorella vulgaris* cells to adsorb cobalt ions, which are heavy metal ions that may be present in effluents from battery manufacturing processes. This study further investigates the capacity of cobalt-adsorbed algal cells to take up amine-functionalized $MgFe_2O_4$ nanoparticles onto their cell walls and to facilitate sedimentation within a magnetic field. This approach could enable the development of an innovative and environmentally friendly method for the removal of heavy metals from industrial wastewater in a more cost-effective manner, thereby complementing conventional wastewater treatment technologies. The interactions between microalgal cells and magnetic nanoparticles were analysed by scanning electron microscopy (SEM), with particular attention to identifying the functional groups involved by Fourier transform

 doi:10.20944/preprints202505.0828.v1

infrared spectroscopy (FTIR) measurements. The particle size and morphology of the magnetic nanoparticles were characterized by HRTEM. Additionally, zeta potential measurements were conducted to examine the separation mechanism of *C. vulgaris* microalgae facilitated by synthesized iron oxide magnetic particles.

2. Results

2.1. Characterization of the amine functionalized magnesium ferrite nanoparticles

In addition to the surface polarity, the sorption capacity of the adsorbents is highly dependent on their specific surface area, and therefore a specific surface area (SSA) determination was performed. Thus, CO_2 adsorption-desorption measurements were carried out at 273 K based on Dubinin-Astakhov (DA) method to determine SSA. The surface area of the $MgFe_2O_4$-NH_2 sample was 54.4 $m^2\ g^{-1}$, which is similar to previously published results (SA_{BET}: 47 $m^2\ g^{-1}$ and 56.5 $m^2\ g^{-1}$) [28]

Particle size and the morphology of the magnetic nanoparticles were examined by HRTEM. On the HRTEM images, spherical ferrite nanoparticles are visible, these aggregated spheres build up from individual, 7-10 nm size nanoparticles (Figure 1 A and B). The particle size histogram was made based on the HRTEM images (by use scalebar) of the amine functionalized $MgFe_2O_4$ samples using ImageJ image analyser software (Figure 1 C). The average diameter of the aggregated spheres is 38 ± 8 nm. To identifying the individual particles, was used selected area electron diffraction (SAED) technique (Figure 1 D). The d-spacing values obtained from the evaluation of the SAED images show excellent correlation with the lattice plane spacings determined for magnesium ferrite based on an X-ray database (PDF 36-0398). To confirm that no other crystalline phases next to magnesium ferrite were present in the sample, XRD measurements were performed (Figure 1 E). Only reflections characteristic of $MnFe_2O_4$ spinel were observed on the XRD diffractogram. The Miller indices associated with the reflections were naturally the same as those marked on the SAED image. The XRD pattern of the sample (Figure 1 C) revealed peaks of only magnesium ferrite, located at (2Th/hkl) 18.2°/(111), 30.1°/(220), 35.4°/(311), 43.1°/(400), 53.4°/(422), 56.9°/(511) and 62.6°/(440), matching to PDF 36–0398 card. Other phases as residue were not detected, therefore, it can be stated that the synthesis method was applicable preparation of pure spinel phase nanoparticles. In the energy dispersive X-ray (EDS) spectrum, bands can be identified that correspond to the chemical elements that make up magnesium ferrite, namely oxygen, iron and magnesium (Figure 1 F). The presence of copper and carbon in the EDS image can be explained by the presence of these elements in the sample holder material (Copper grid, lacey carbon). The presence of carbon is also due to the adsorption of the organic compounds used in the synthesis (ethylene glycol and monoethanol amine) on the surface of the particles.

 doi:10.20944/preprints202505.0828.v1

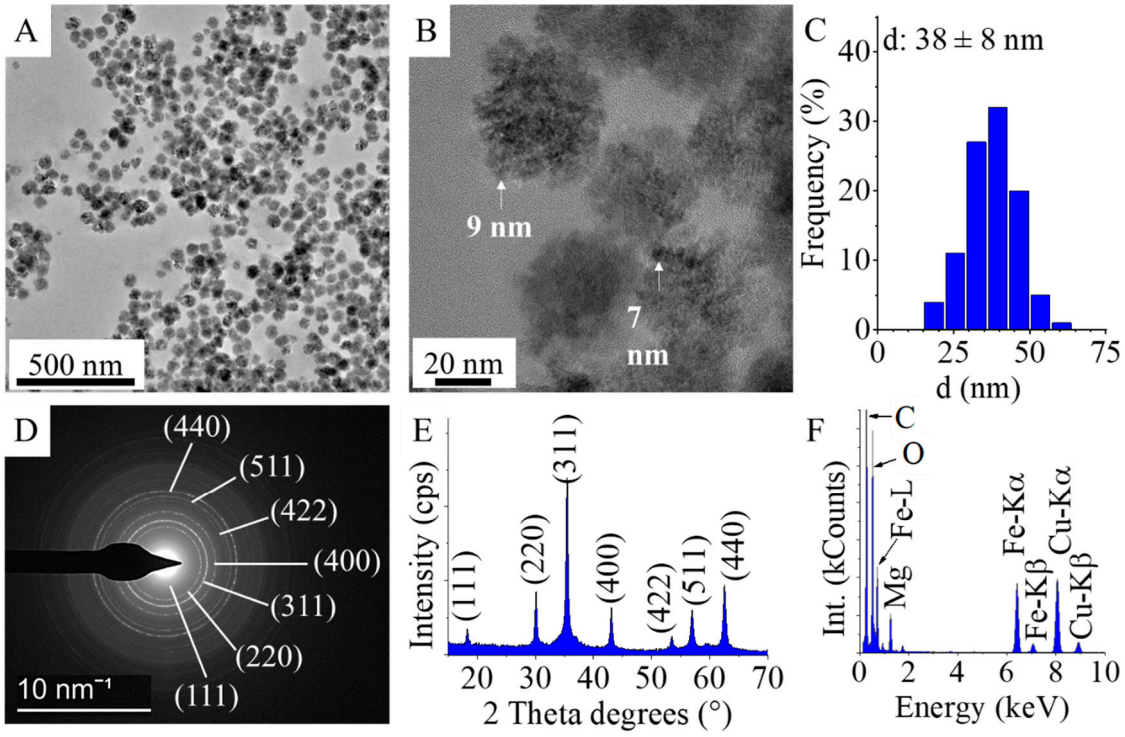

Figure 1. HRTEM pictures (A and B), size distribution (C), SAED picture (D), XRD pattern (E), and EDS (F) of the amine functionalized $MgFe_2O_4$ nanoparticles

In order to understand the adsorption interactions between algae and magnetic nanoparticles, it is important to identify the functional groups on the surface of the particles, thus Fourier transformation infrared spectroscopic measurement was carried for confirm the presence of the -NH_2 and -OH groups. Two characteristic bands are observed onto he spectrum of $MgFe_2O_4$ at 564 cm^{-1} and 621 cm^{-1} wavenumbers, which are assigned to intrinsic stretching vibration modes of the metal-oxygen bonds (νM-O) at the octahedral and tetrahedral sites [29] (Figure 2 A). The bands corresponding to the stretching vibration modes of C-N and C-O bonds at 1052 cm^{-1} and 876 cm^{-1} wavenumbers, which are originated from the amine (-NH_2) and hydroxyl (-OH) groups. Other absorption band was identified at 1365 cm^{-1} which can belong to the OH bending vibrations, respectively. The band of bending vibration mode of the N–H bonds was found at 1610 cm^{-1} wavenumber, it corresponds to the free amine functional groups, moreover the presence of adsorbed water molecules may also contribute significantly to this band as shoulder at 1638 cm^{-1}. The symmetric and asymmetric stretching vibration of the aliphatic and aromatic C-H bonds resulted in absorption at 2870 cm^{-1} and 2941 cm^{-1}, which can be explained by the adsorbed organic molecules (EG and EA) on the surface [30,31]. The stretching vibration bands of the hydroxyl and amine groups are overlapping and result in a broad region between 3000 cm^{-1} and 3750 cm^{-1}.

Zeta potential (ZP)measurements were carried out at ambient pH in distilled water (pH: 6). The surface hydroxyl groups are partially found in a deprotonated form, resulting in negative ZP (-5.6 ± 4.3 mV) (Fig. 2 B). Next to the -OH groups, -NH_2 functional groups are found on the nanoparticles, which can become protonated when the pH decreases, leading to the appearance of positive charges (-NH_3^+). Due to the positive charges formed as a result of the protonation of the amine groups, negatively charged algae can form an eletrostatic interaction with the magnetic nanoparticles.

 doi:10.20944/preprints202505.0828.v1

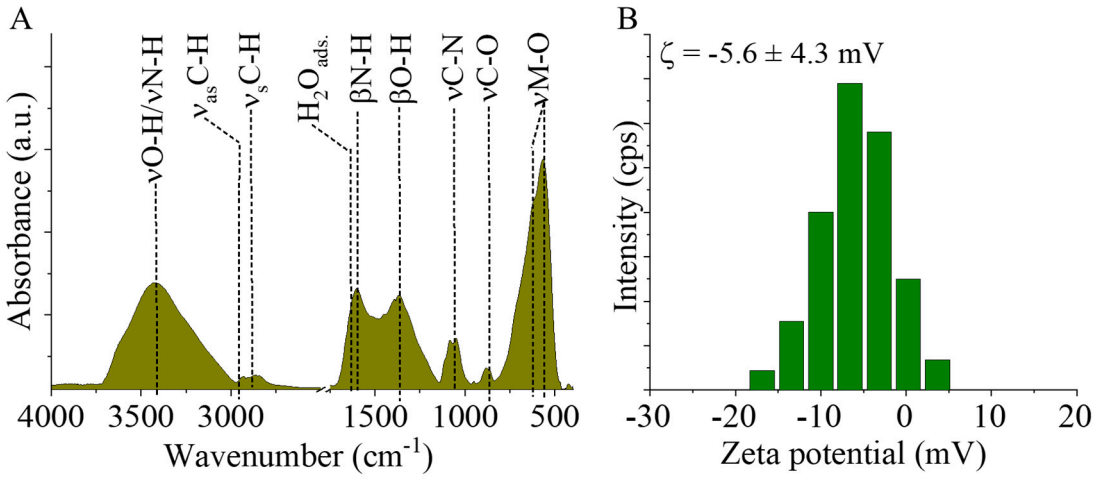

Figure 2. FTIR spectra (A) and zeta potential distribution diagram (B) of the $MgFe_2O_4$-NH_2.

For characterization of the magnetic behaviour of the amine functionalized $MgFe_2O_4$ sample was carried VSM measurement at room temperature. The magnetic saturation (Ms) of sample was 39 Am^2/kg at 150,000 A/m magnetic field (Figure 3). In the case of $MgFe_2O_4$ nanoparticles, similar Ms values (Ms: 12-32 Am^2/kg) have been reported in other literatures [32–34]. Our Ms value is higher than the reported Ms value of 27 Am^2/kg at room temperature for bulk magnesium ferrite [35]. On the magnetization curve is visible narrow hysteresis loop with low coercivity (Hc: 955 A/m) and low remanent magnetization (Mr: 1.3 Am^2/kg) which are relatively small values, that indicate the soft magnetic nature of the synthesized particles at room temperature [36]. Narrow hysteresis loops also indicate that the prepared samples can be easily demagnetized as clearly shown in the photograph in Figure 3.

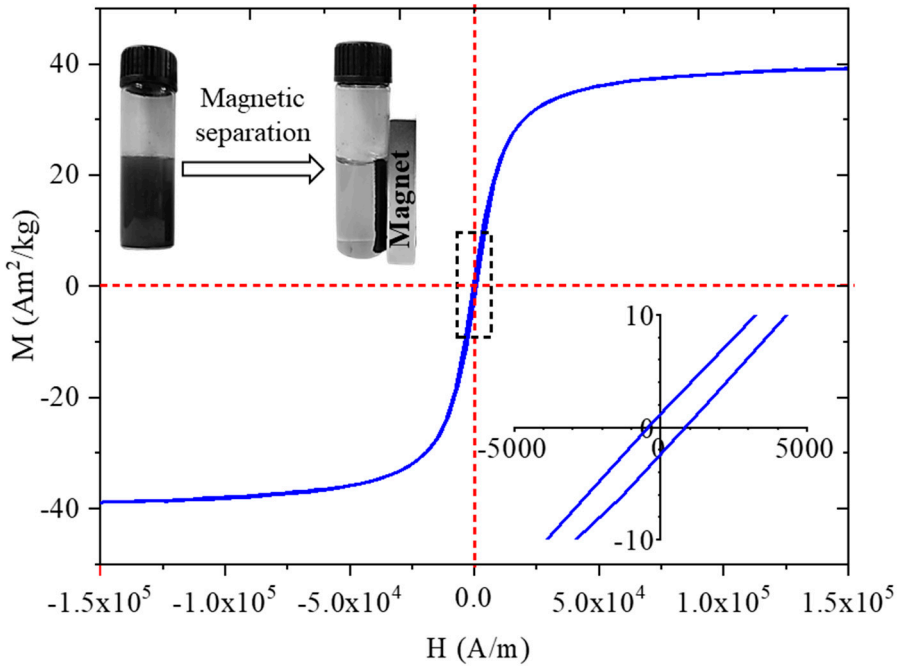

Figure. 3. VSM curve and picture of the magnetic separation of the $MgFe_2O_4$-NH_2

2.2. Results of the cobalt adsorption tests by using of Chlorella vulgaris

After the addition of the cobalt stock solution, the culture Co2+ was rapidly removed by the *C. vulgaris* cells. The initial concentration of Co2+ in the medium was 63.6 mg/l, which decreased to 2.49

 doi:10.20944/preprints202505.0828.v1

mg/l within 30 minutes. This represents a removal efficiency of 96.44%. The Co2+ concentration in the medium continued to decrease and after ten hours of cobalt addition, 1.01mg/l Co2+ was detected in the cell free supernatant, giving a removal efficiency of 98.78%.
Chlorella cells were observed by light microscopy before and after cobalt treatment which revealed severe deterioration of cell morphology. Cells became extremely swelled, lot of cells showed necrotic morphology with vanished cytoplasm, and cell debris (Fig.4).

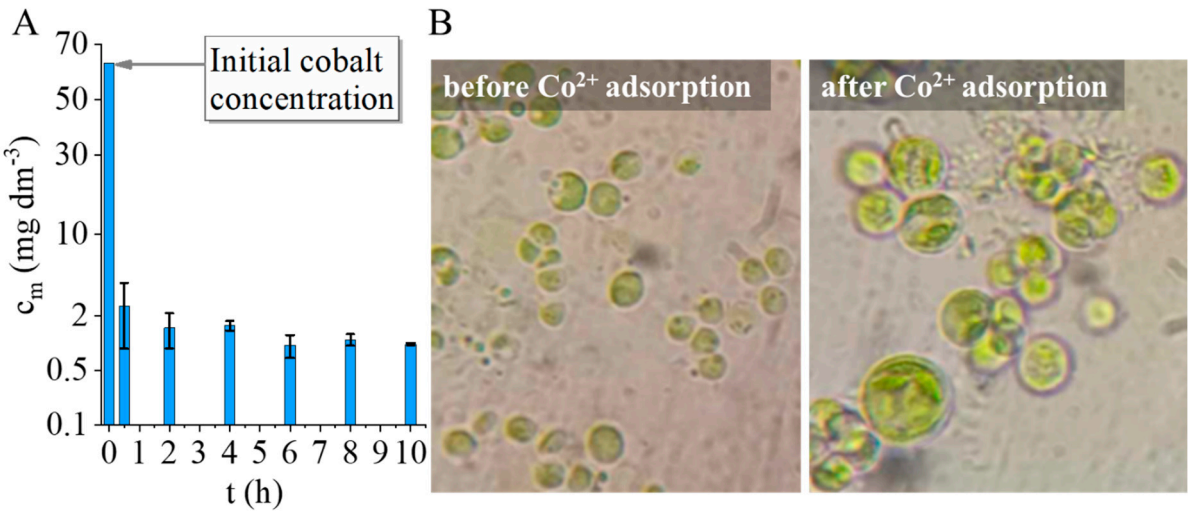

Figure 4. Cobalt adsorption by *Chlorella vulgaris*, cobalt concentration vs. contact time (A), optical microscopic images from the algae before and after cobalt adsorption (B)

Under the influence of the magnetic field, the algal biomass bound to the $MgFe_2O_4$ magnetic nanoparticles is completely separated from the nutrient solution within 60 sec. There is no significant difference between the separation rate of cobalt adsorbed algal biomass and normal biomass. For normal algal biomass at a concentration of 3.6 g/l, the optical density at 680 nm decreased from 2,432 to 0,123, representing 94,9 % HE%, and for cobalt adsorbed algal biomass, the optical density decreased from 2,226 to 0,102, representing 95.4 % HE%. Magnetic separation of algal biomass of different concentrations is achieved with high efficiency in 60 s, despite the low concentration of magnetizable nanoparticles compared to the concentration of algal suspensions. The optical density at 680 nm of the algal biomass decreases from 2,432 to 0,111 for the highest concentration algae suspension, with 95,4 % of the biomass harvested. The optical density of the algal biomass decreases from 1,031 to 0,008 for the lowest concentration algae suspension, with 99,2 % HE% (Fig.5). It is expected that the separation efficiency of the higher concentration algal suspension would increase with the concentration of the nanoparticles.

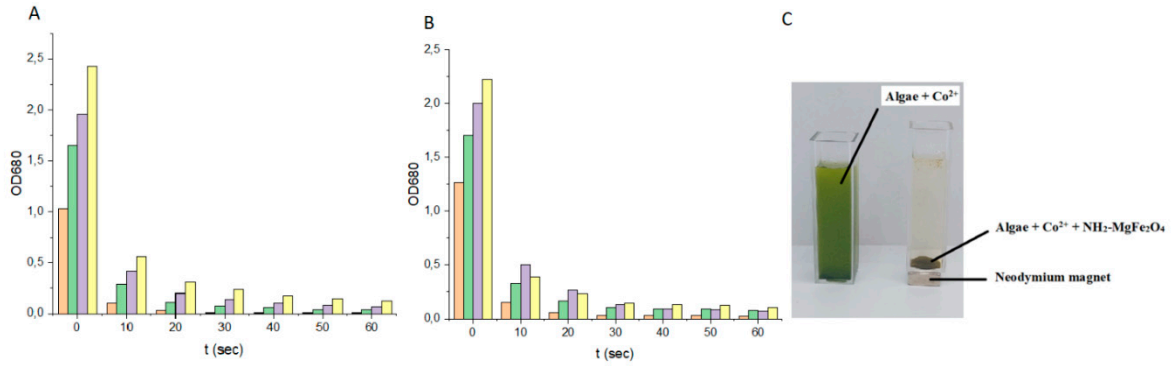

 doi:10.20944/preprints202505.0828.v1

Figure 5. Magnetic separation of normal Chlorella vulgaris (A) and cobalt adsorbed *Chlorella vulgaris*, intensity variation of UV-VIS spectra at different times (B), images from algae before and after magnetic separation (C).

We have performed electron microscopy of algae that were magnetically separated from the aqueous medium after cobalt adsorption using magnesium ferrite nanoparticles. The TEM image clearly shows the $MgFe_2O_4$ magnetic nanoparticles evenly distributed on the surface of the algae (Fig. 6 A). The magnesium ferrite particles with bright and sharp contrast are clearly visible on the high-angle annular dark-field (HAADF) image (Fig. 6 B). The carbon sign on the elemental maps clearly shows the location of the algae, which have a uniform distribution of adsorbed cobalt ions on their surface. The elemental maps also identify magnesium, iron and oxygen, which are components of magnesium ferrite. By comparing the positions of magnesium and iron on the elemental maps, it can be observed that magnesium is also enriched where no sign of iron is visible. This can be explained using magnesium sulphate as a nutrient source during algal growth.

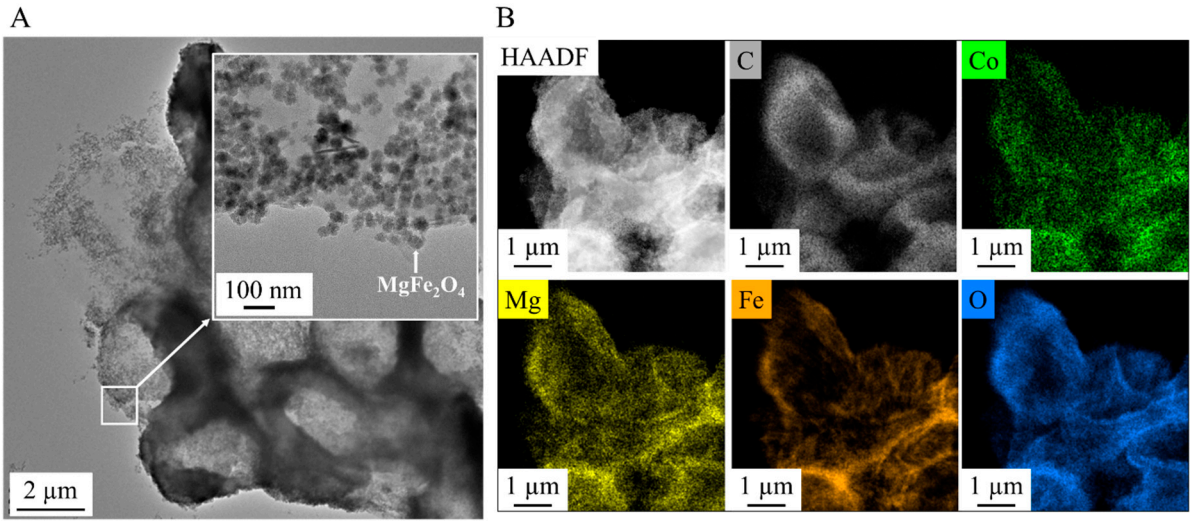

Figure 6. TEM pictures of the algae and the nanoparticles (A) and element maps of the algae after cobalt adsorption and magnetic separation (B).

3. Discussion

The study demonstrates the successful synthesis and characterization of amine-functionalized magnesium ferrite ($MgFe_2O_4$) nanoparticles, which consist of aggregated spheres made up of 7–10 nm particles. Fourier transform infrared spectroscopy (FTIR) confirmed the presence of -NH_2 and -OH functional groups, crucial for surface reactivity. Zeta potential measurements at neutral pH revealed a slightly negative charge (-5.6 ± 4.3 mV), indicating the partial deprotonation of surface hydroxyl groups. However, at lower pH levels, protonation of the -NH_2 groups leads to positive surface charges, facilitating electrostatic interactions with negatively charged algae. The nanoparticles exhibited strong magnetic properties, with a saturation magnetization (Ms) of 39 Am^2/kg at 150 000 A/m, confirmed by vibrating sample magnetization (VSM). This property was key to the efficient separation of algae, which bound to the nanoparticles through electrostatic interactions. The algae exhibited high cobalt adsorption efficiency, reducing the Co^{2+} concentration from 63.6 mg/L to 2.49 mg/L within 30 min, achieving a removal efficiency of 96.44%, which further increased to 98.78% after 10 h. When exposed to a magnetic field, the algal biomass attached to the $MgFe_2O_4$ magnetic nanoparticles was separated from the nutrient solution with an efficiency of 94.9-99.2% within 60 seconds. The separation rate was comparable for both cobalt-adsorbed and unmodified algal biomass, with no significant difference between the two. TEM analysis confirmed the even distribution of nanoparticles on the algal surfaces after magnetic separation.

 doi:10.20944/preprints202505.0828.v1

These results highlight the potential of low-cost, biocompatible, and widely available magnetic nanoparticles in wastewater treatment, particularly for the removal of heavy metals, offering a promising approach for sustainable environmental remediation.

4. Materials and Methods

4.1. Materials

The amine-functionalized magnesium ferrite nanoparticles were synthesized from magnesium nitrate hexahydrate, $Mg(NO_3)_2 \cdot 6H_2O$, MW: 290.79 g/mol (ThermoFisher GmbH, D-76870 Kandel, Germany) and iron(III) nitrate nonahydrate, $Fe(NO_3)_3 \cdot 9H_2O$, MW: 404.00 g/mol (VWR Int. LtD., B-3001 Leuven, Belgium). Ethylene glycol, $HOCH_2CH_2OH$, (VWR Int. Ltd., F-94126 Fontenay-sous-Bois, France) was used as dispersion media. For coprecipitation and the functionalization of the ferrites, monoethanolamine, NH_2CH_2OH (Merck KGaA, D-64271 Darmstadt, Germany) and sodium acetate, CH_3COONa (ThermoFisher GmbH, D-76870 Kandel, Germany) were used.

4.2. Synthesis of the amine functionalized magnesium ferrite nanoparticles

Synthesis of the magnetic particles was carried based on the method of Nonkumwong et al. [25]. Sodium acetate (15 mmol) was dissolved in ethylene glycol (10 ml) and heated to 100 °C during continuous stirring. Magnesium(II)-nitrate (1 mmol) and iron(III)-nitrate (2 mmol) precursors were solved in 50 mL ethylene glycol, after complete dissolution, the two solutions were combined. The mixture was stirred for 30 minutes, then ethanolamine (4 mL) was added. The solution was heated to 200 °C and refluxed for 12 hours with continuous stirring. The dispersion was cooled down to room temperature, then it was separated by magnetic field use of Nd magnet. The solid phase was washed with distilled water several times. Finally, the ferrite was dried 85 °C overnight.

4.3. Cobalt adsorption tests

The *Chlorella vulgaris* strain was obtained from the Advanced Materials and Intelligent Technologies Higher Education and Industrial Cooperation Centre at the University of Miskolc.

C. vulgaris strain was maintained in modified “endo” medium [26] containing KNO_3 3g/l, KH_2PO_4 1.2g/l, $MgSO_4 \cdot 7H_2O$ 1.2gl/l, citric acid 0.2 g/l, $FeSO_4 \cdot 7H_2O$ 0.016 g/l, $CaCl_2 \cdot 2H_2O$ 0.105g/l, trace element stock solution 1ml/l. For trace elements a stock solution has been prepared containing Na_2EDTA 2.1g/l, H_3BO_3 2.86g/l, $ZnSO_4 \cdot 7H_2O$ 0.222 g/l, $MnCl_2 \cdot 4H_2O$ 1.81 g/l, $Na_2MoO_4 \cdot 2H_2O$ 0.021g/l, and $CuSO_4 \cdot 5H_2O$ 0.07g/l. After solution of all components of the medium the pH was adjusted to 6.5±0,2 and the temperature was controlled at 24 °C.

For growing of *C. vulgaris* a glass tubular air lift photo-bioreactor system was constructed, which consisted of Hailea V20 membrane compressor with a capacity of 20 l/min air flow with electric power 15W. The reactor system contained 9 pieces of glass vessel with a volume of 500 ml. The air flow rate was 4,5 l/min in each reactor vessel. Reactors were illuminated with. LED lamps with a light intensity of 3000 lumen. The reactors were inoculated with 4.2 mg/l concentrated Chlorella v. culture at a 1% inoculation rate. The initial biomass concentration at inoculation was 0.9 mg/l (= 0.5±0.1 OD680) in the reactor vessels. Cell growth was followed by measuring of OD680 values by UV-6300PC Doublebeam Spectrophotometer of the samples by 24 hours.

A cobalt solution (Certipur, Merck Ltd.) with a concentration of 60 mg/l is added to the bioreactors at the 24. hour of cultivation. 3 ml samples were taken from the cultures after 30 min of cobalt addition and after 2, 4, 6, 8 and 10 hours. A solution of cobalt at a concentration of 60 mg/L was selected as it represents the toxicity limit for Chlorella vulgaris [27].

 doi:10.20944/preprints202505.0828.v1

For Co^{2+} analysis cell free supernatant was prepared by centrifugation of cultures in Eppendorf tubes with 9000 g; 10 min. 1ml supernatants were transferred to 15 ml Falcon tubes and were diluted to 10 ml with ultrapure water.

4.4. Magnetic separation tests of the cobalt adsorbed algae

In the experiments, the time and efficiency of magnetic separation were compared between cobalt adsorbed algal biomass and normal algal biomass under different algal concentrations. Concentrated *Chlorella v.* culture containing 4,2 mg/l dry biomass was diluted. Different concentrations of algal suspension were used: 3,6 mg/l (= 2,0±0,1 OD680), 2,7 mg/l (= 1,5±0,1 OD680), 1,8 mg/l (= 1,0±0,1 OD680), 0,9 mg/l (= 0,5±0,1 OD680), while the concentration of NH_2-Fe_2O_4 solution was fixed at 0.511 g/l. 100 cm^3 algal suspension of different concentrations was mixed with 0,511 g/l of amine-functionalized $MgFe_2O_4$ nanoparticles for 10 min using the air bubbling compressor by Hailea V20 membrane compressor with a capacity of 20 l/min air flow with electric power 15W. An additional 100 cm^3 algal suspension of different concentrations a cobalt solution of 60 mg/l was added, and it was mixed with air bubbling for 30 min. Subsequently, the algal biomass was treated with amine-functionalized $MgFe_2O_4$ nanoparticles at a concentration of 0.511 g/l for 10 min using the air bubbling compressor. The pH was adjusted to 6,5 with phosphate buffer and the temperature was 24 °C.

4.5. Characterization Technics

For morphological characterisation and size analysis of the magnetic nanoparticles were carried by use High-resolution transmission electron microscopy (HRTEM, Talos F200X G2 electron microscope with field emission electron gun, X-FEG, accelerating voltage: 20-200 kV, ThermoScientific, Waltham, MA, USA). For the imaging and selected area electron diffraction (SAED), SmartCam digital search camera (Ceta 16 Mpixel, 4k x 4k CMOS camera, Thermo Scientific, Wal-tham, MA, USA) was used with a high-angle annular dark-field (HAADF) detector. During sample preparation, the aqueous dispersion of the nanoparticles was dropped onto copper grids (Ted Pella Inc., 4595 Redding, CA 96003, USA). For phase analysis of the magnetic nanoparticles, X-ray diffraction (XRD) method and Rietveld refinement were applied. For X-ray diffraction measurements Bruker D8 diffractometer (Cu-Kα source) in parallel beam geometry (Göbel mirror) with Vantec detector was used. The functional groups on the surface of the amine-functionalized magnesium ferrite were examined with Fourier-transform infrared spectroscopy (FTIR), using a Bruker Vertex 70 spectroscope. The measurements were carried out in transmission mode, whereas the sample preparation was carried with palletisation in spectroscopic potassium bromide (10 mg ferrite sample was measured to 200 mg KBr). The zeta potential of the nanoparticles was measured based on electrophoretic mobility by applying laser Doppler electrophoresis with a Malvern Zetasizer Nano ZS equipment (Malvern Panalytical, Malvern, UK). The specific surface area (SSA) of the samples was measured by carbon dioxide adsorption-desorption experiments at 273 K based on Dubinin-Astakhov (DA) method (with Micromeritics ASAP 2020 equipment). To measure the saturation magnetization (Ms), remained magnetization (Mr) and the coercivity (Hc) of the samples was carried out with vibrating-sample magnetometer (VSM) system based on a water-cooled Weiss-type electromagnet (self-developed magnetometer by University of Debrecen). For the VSM test the sample was pelletized with mass of 20 mg. The magnetization (M) was measured as a function of magnetic field (H) up to 150,000 A/m field strength at room temperature.

The concentration of cobalt ions in the supernatant was determined by Inductively coupled plasma atomic emission spectrometry (ICP-AES). The ICP instrument was the Varian-make 720 ES type simultaneous, multielement spectrometer with axial plasma view. The parameters of the analyses were the following: Running frequency of the RF generator 40[MHz]; Sample introduction device: V-groove nebulizer with sturman-masters spray chamber; sample uptake 2.1 cm^3/min. Length of signal integration: 8s; number of reading: 3/sample. The calibration of the instrument was

 doi:10.20944/preprints202505.0828.v1

performed by using a solution series prepared from a 1000 mg/dm^3 monoelement stock cobalt solution (Certipur, Merck Ltd.)

Co^{2+} removal efficiency was calculated by the following equation:

$$\textit{Removal efficiency \%} = \frac{[Co^{2+}]_{t0} - [Co^{2+}]_{t1}}{[Co^{2+}]_{t0}} \text{x}100$$

$[Co^{2+}]_{t0}$ = initial concentration of Co^{2+} given in mg/L,
$[Co^{2+}]_{t1}$ = Co^{2+} concentration of the given time point after cobalt addition of the cell free supernatant.

To determine the efficiency of nanoparticles to bind to the surface of cobalt adsorbed algal cells and normal algal cells, we measured their sedimentation rate in a magnetic field. 4 ml of the algal suspension was measured into a special cuvette with a 10×10×3 mm, N45 neodymium magnet glued to the bottom. The cuvette with the magnet was placed in the spectrophotometer cuvette holder and the sedimentation rate was measured by the change in optical density over time. The change in optical density was followed by measuring at 680 nm by UV1100/UV-1200 Doublebeam spectrophotometer (Frederiksen).

The harvesting efficiency (HE%) of the process was calculated from Equation:

$$\textit{HE \%} = \frac{OD_0 - OD_1}{OD_0} \times 100$$

OD_0 = initial absorbance of the microalgae cultivation at a wavelength of 680 nm,

OD_1 = absorbance at the same wavelength of the supernatant liquid that separates from the microalgae-particles flocs after the application of the magnetic field.

Abbreviations

HRTM	High-Resolution Transmission Electron Microscopy
FTIR	Fourier Transform Infrared Spectroscopy
SEM	Scanning Electron Microscopy
VSM	Vibrating Sample Magnetometry
NMC	*Nickel Manganese Cobalt Oxide*
NCA	Nickel Cobalt Aluminum Oxide
LMO	*Lithium Manganese Oxide*
PDDA	poly diallyldimethylammonium chloride
PEI	polyethylenimine
APTES	3-aminopropyl triethoxysilane
SAED	Selected Area Electron Diffraction
HAADF	High-Angle Annular Dark-Field
ICP-AES	Inductively Coupled Plasma Atomic Emission Spectrometry

 doi:10.20944/preprints202505.0828.v1

References

1. Battery University: https://batteryuniversity.com/article/bu-205-types-of-lithium-ion 2023., (Date of download: 07.11.2024.)
2. P.B. Tchounwou, C.G. Yedjou, A.K Patlolla,D.J. Sutton: Heavy metal toxicity and the environment, *PubMed Central*, **2012**.; 101: 133–164.
3. Gunatilake SK. Methods of Removing Heavy Metals from Industrial Wastewater. *Journal of Multidisciplinary Engineering Science Studies* (JMESS), **2015.**, ISSN: 2912-1309
4. Barakat MA. New trends in removing heavy metals from industrial wastewater. *Arabian Journal of Chemistry*. **2011**.;4(4):361-377. doi:10.1016/j.arabjc.2010.07.019
5. Noman EA, Ali Al-Gheethi A, Al-Sahari M, et al. An insight into microelectronics industry wastewater treatment, current challenges, and future perspectives: a critical review. *Applied Water Science*. **2024**.;14(4). doi:10.1007/s13201-024-02104-7
6. Ribeiro C, Scheufele FB, Espinoza-Quiñones FR, et al. A comprehensive evaluation of heavy metals removal from battery industry wastewaters by applying bio-residue, mineral and commercial adsorbent materials. *Journal of Materials Science*. **2018.**;53(11):7976-7995 doi:10.1007/s10853-018-2150-6
7. Balzano S, Sardo A, Blasio M, et al. Microalgal Metallothioneins and Phytochelatins and Their Potential Use in Bioremediation. *Frontiers in Microbiology*. **2020.**;11. doi:10.3389/fmicb.2020.00517
8. Dewi ERS, Nuravivah R. Potential of Microalgae Chlorella vulgaris As Bioremediation Agents of Heavy Metal Pb (Lead) On Culture Media. In: E3S Web of Conferences. *EDP Sciences*; **2018.** Vol 31. doi:10.1051/e3sconf/20183105010
9. Junran Je, Cuiqiyun Yang, Luojia Xia: Protoplast Preparation for Algal Single-Cell Omics Sequencing, *Microorganisms*, **2023.** 1(2):538
10. Anikó Kőnig-Péter, Ferenc Kilár, Attila Felinger, Tímea Pernyeszi: Biosorption characteristics of Spirulina and Chlorella cells to accumulate heavy metals *Journal of the Serbian Chemical Society*, **2014.**, Paper 5988-EC,
11. F. Veglio, F. Beolchini, Removal of metals by biosorption: A review, *Hydrometallurgy*, **1997.**, 301-316.
12. Ahalya N, Ramachandra T v, Kanamadi RD. Biosorption of Heavy Metals *Research Journal Of Chemistry And Environment*, **2003.**, 7 (4), 71-79
13. A. Abdelfattah, S. S. Ali, H. Ramadan, E. I. El-Aswar, R. Eltawab, Shih-Hsin Ho, T. Elsamahy, S. Li, M. M El-Sheekh, M. Schagerl, M. Kornaros, J. Sun: Microalgae-based wastewater treatment: Mechanisms, challenges, recent advances, and future prospects *Environmental Science and Ecotechnology*, **2023.**,13(6):100205
14. Abo Markeb A, Llimós-Turet J, Ferrer I, Blánquez P, Alonso A, Sánchez A, Moral-Vico J, Font X. The use of magnetic iron oxide based nanoparticles to improve microalgae harvesting in real wastewater. *Water Research,* **2019.,** 1;159:490-500. doi: 10.1016/j.watres.2019.05.023
15. Prochazkova G, Podolova N, Safarik I, Zachleder V, Branyik T. Physicochemical approach to freshwater microalgae harvesting with magnetic particles. *Colloids Surf B Biointerfaces*. **2013**., Dec 1;112:213-8. doi: 10.1016/j.colsurfb.2013.07.053.
16. Lee H, Suh H, Chang T. Rapid removal of green algae by the magnetic method. *Environmental Engineering Research*. **2012**.;17(3):151-156. doi:10.4491/eer.2012.17.3.151
17. Eroglu, E.; Agarwal, V.; Bradshaw, M.; Chen, X.; Smith, S.M.; Raston, C.L.; Swaminathan Iyer, K. Nitrate removal from liquid effluents using microalgae immobilized on chitosan nanofiber mats. *Green Chem.*, **2012**., 14, 2682–2685.
18. Hu,Y.R.; Guo, C.; Wang, F.; Wang, S.K.; Pan, F.; Liu, C.Z. Improvement of microalgae harvesting by magnetic nanocomposites coated with polyethylenimine. *Chem. Eng. J.*, **2014**., 242, 341–347.
19. Prochazkova, G.; Podolova, N.; Safarik, I.; Zachleder, V.; Branyik, T. Physicochemical approach to freshwater microalgae harvesting with magnetic particles. *Colloids Surf. B: Biointerfaces,* **2013**., 112, 213–218.
20. Prochazkova, G.; Safarik, I.; Branyik, T. Harvesting microalgae with microwave synthesized magnetic microparticles. *Bioresour. Technol.*, **2013**., 130, 472–477.
21. Xu,L.;Guo,C.; Wang, F.; Zheng, S.; Liu, C.Z. A simple and rapid harvesting method for microalgae by in situ magnetic separation. *Bioresour. Technol.*, **2011**., 102, 10047–10051.

 doi:10.20944/preprints202505.0828.v1

22. Fraga-Garcia, P.; Kubbutat, P.; Brammen, M.; Schwaminger, S.; Berensmeier, S. Bare iron oxide nanoparticles for magnetic harvesting of microlagae: From interaction behavior to process realization. *Nanomaterials*, **2018.**, 8, 292.
23. Ilosvai ÁM, Gerzsenyi TB, Sikora E, et al. Simplified Synthesis of the Amine-Functionalized Magnesium Ferrite Magnetic Nanoparticles and Their Application in DNA Purification Method. *International Journal of Molecular Sciences*, **2023**.;24(18). doi:10.3390/ijms241814190
24. C. Aoopngan *et al.*, "Amine-Functionalized and Hydroxyl-Functionalized Magnesium Ferrite Nanoparticles for Congo Red Adsorption," *ACS Appl. Nano Mater.*, **2019**., vol. 2, no. 8, pp. 5329–5341 doi: 10.1021/ACSANM.9B01305/SUPPL_FILE/AN9B01305_SI_001.PDF.
25. Q. Xu *et al.*, "Heterotrophically Ultrahigh-Cell-Density Cultivation of a High Protein-Yielding Unicellular Alga Chlorella With a Novel Nitrogen-Supply Strategy," *Front. Bioeng. Biotechnol.*, **2021**., vol. 9,pp. 1–9 doi: 10.3389/fbioe.2021.774854.
26. Fathi AA, Afkar E, Ababna H. Toxicological Response of the Green Alga Chlorella Vulgaris, to Some Heavy Metals, *American Journal of Environmental Sciences*, **2010.**, Vol 6.
27. J. Nonkumwong, S. Ananta, and L. Srisombat, "Effective removal of lead(II) from wastewater by amine-functionalized magnesium ferrite nanoparticles," *RSC Adv.*, **2016.**, vol. 6, no. 53, pp. 47382–47393 doi: 10.1039/C6RA07680G.
28. Zhou B, Zhang YW, Liao CS, Yan CH, Chen LY, Wang SY. Rare-earth-mediated magnetism and magneto-optical Kerr effects in nanocrystalline CoFeMn0.9RE0.1O4 thin films, *Journal of Magnetism and Magnetic Materials*, **2004**. ;280(2-3):327-333. doi:10.1016/J.JMMM.2004.03.031
29. Wang, H., Su, W., and Tan, M. (2020a). Endogenous Fluorescence Carbon Dots Derived from Food Items. *The Innovation*, **2020.**, 1 (1), 100009. doi:10.1016/j.xinn.2020.04.009
30. Bruce IJ, Taylor J, Todd M, Davies MJ, Borioni E, Sangregorio C, Sen T (2004) Synthesis, characterisation and application of silica-magnetite nanocomposites. J Magn Magn Mater 284:145–160. doi:10.1016/J.JMMM.2004.06.032.
31. Aslibeiki, B.; Varvaro, G.; Peddis, D.; Kameli,P. *J. Magn.and Magn. Mater.* **2017,** *422,* 7–12. doi:10.1016/j.jmmm.2016.08.057
32. Araújo, J.; Araujo-Barbosa, S.; Souza, A. L. R. Tuning structural, magnetic, electrical, and dielectric properties of MgFe2O4 synthesized by sol-gel followed by heat treatment. *J. Phys. Chem. Solids* **2021**, *154*, 110051 DOI: 10.1016/j.jpcs.2021.110051
33. M. Z. Naik and A. V. Salker,: Tailoring the super-paramagnetic nature of $MgFe_2O_4$ nanoparticles by In3+ incorporation, *Mater. Sci. and Eng. B*, **2016.**, vol. 211, pp. 37–44 doi: 10.1016/j.mseb.2016.05.019.
34. R. G. Kulkarni and H. H. Joshi, "Comparison of Magnetic Properties of MgFe2O4 Prepared by Wet-Chemical and Ceramic Methods," *Journal of Solid State Chemistry*, **1986.**, Vol. 64, No. 2, pp. 141-147. doi:10.1016/0022-4596(86)90133-7
35. Naaz, F., Dubey, H.K., Kumari, C. *et al.* Structural and magnetic properties of $MgFe_2O_4$ nanopowder synthesized via co-precipitation route. *SN Appl. Sci.* **2020**. **2**, 808 doi: 10.1007/s42452-020-2611-9